Research Article

Journal of Applied Material Science & Engineering Research

Study of UV Stability and Physical Properties of Jute/Soy Flour Green Nanocomposites

Murshid Iman, Moon Mandaland and Tarun K Maji*

Department of Chemical Sciences, Tezpur University, Assam - 784028, India

***Corresponding author**
Tarun K Maji, Department of Chemical Sciences, Tezpur University, Assam - 784028, India, Tel: +91 3712 267007; Extn: 5053; Fax: +91 3712 267005; E-mail: tkm@tezu.ernet.in

Submitted: 22 Dec 2017; **Accepted**: 30 Dec 2017; **Published**: 02 Feb 2018

Abstract

Glutaraldehyde cross-linked jute fabric and soy flour was used to develop green nanocomposites via solution-induced intercalation method. The effect of TiO_2 alone (TNP) and TiO2 in combination with nanoclay on the properties of the nanocomposites was studied. Fourier transfer infrared spectroscopy (FT-IR), scanning electron microscopy (SEM), X-ray diffractrometry (XRD), and transmission electron microscopy (TEM) were used to examine the structural and morphological properties. They clearly revealed that both TNP and nanoclay were successfully loaded into the composite. The thermal and mechanical properties were determined using thermo gravimetric analysis (TGA), and mechanical tests, respectively. The study discloses noteworthy changes in the observed properties of the composites with inclusion of nanoparticles. Furthermore, in comparison to the unfilled composites, nanoparticles filled ones were found to exhibit much improved UV-resistance, flame retarding properties, and dimensional stability. The study revealed a strong interfacial interaction between the filler and the matrix within the prepared green nanocomposites.

Keywords: Jute, Soy flour, TiO_2, Compression molding, Green nanocomposites, UV-Resistance study Mechanical properties, Thermal properties.

Abbreviations

TNP- TiO_2 nanoparticles
GA- glutaraldehyde
SF- soy flour
J- Jute
SF/J- soy flour/ jute composite
SF/J/GA/T- soy flour/ jute/ TiO_2 nanocomposites
SF/J/GA/T/N- soy flour/ jute/ TiO_2/ nanoclay nanocomposites

Introduction

In recent years, the use of bio-based polymer composites have increased immensely due to their several advantages over their synthetic counterparts. They are moving into the mainstream and soon will be competing with synthetic commodities [1]. The fibre developed from plant from drawing much interest as a reinforcing agent improving the thermal and mechanical properties of the composites [2,3]. They are used in various indoor, outdoor applications, and in a number of automobile industries. They are readily available and cheaper and most notably are environmental friendly. Recently, the need for greener technologies based on renewable and eco-friendly materials has attracted the attention of the researchers throughout the globe [4-6].

Out of a number of biopolymers, soy protein, soy flour (SF) is one of the less expensive and easily available polymer [7]. The presence of various polar and reactive amino acids such as arginine, cysteine, lysine and histidine in the structure of SF has allowed them to react with cross linking agent like glutaraldehyde (GA), thereby improving the physical properties of SF [8,9]. Apart from the several benefits, SF based materials have certain drawbacks like poor flexibility and water resistivity. Generally, the flexibility is improved by using plasticizer like glycerol. However, the use of plasticizer also reduces its mechanical strength and lowers water resistivity [10-13]. Thus, bio-fibres have turned out to be a promising alternative for enhancing the mechanical properties of such materials. Bio-fibres display significant features like high specific modulus, low density, easy availability, cost effective and biocompatibility [14]. Application of bio fibres in areas like automobiles, packing materials, furniture, and constructions are now highly demanding. Apart from various natural fibres, jute (J) is one of the cheapest and widely available vegetable fibre, which can be modified into cost-effective and environmentally benign green products [15,16]. Surface modification of jute is essential as it lowers the moisture absorption and enhances the wet ability of the fibre with polymer resulting in improved interfacial bond strength along with better mechanical properties of greener composites [17, 18]. Moreover, the properties of SF/J composites can be improved by using nanomaterials [9]. Out of various nanomaterials predecessors the use of nanoclayis extensive for the synthesis of polymer nanocomposite. Besides using nanoclay, different metal oxide nanoparticles like ZnO, TiO_2, SiO_2 etc. are also used to improve various properties of bio-nanocomposites [19,20]. In outdoor application of biopolymer-based materials, UV protection, flame retardancy and weathering resistance are very vital. Nowadays, TiO_2nanopowderis being used due to various advantages such as

non-toxic, low cost, corrosion resistant, high refractive index, UV filtration capacity, and better hardness. Reinforcement by TiO_2 also improves electrical, optical, and physiochemical properties at a very low TiO_2 concentration, which make polymer TiO_2 nanocomposites a promising new class of materials [21]. There are limited information regarding the study of the effect of nanoparticles on soy flour based composites. There is enough scope to do further work in this area.

The present work aims to study the effect of TNP either or alone and in combination with nanoclay (*i.e*. TiO_2 and TiO_2-nanoclay) on thermal and mechanical properties of SF/J composites. Besides this, their effect on properties like UV resistance, dimensional stability, and flame retardancy of the composites have been studied.

Experimental

Materials

Jute fabrics and soy flour (SF) were purchased from local market, Tezpur, Assam, India. Glutaraldehyde (GA) (61847005001730), benzene, glycerol (61756025001730) and NaOH (68151) pellets were obtained from Merck Private Limited (Mumbai, India). TiO_2nanopowder (< 100 nm) (634662) and Montmorillonite K-10 clay (purity 99.99 %) (281522) were procured from Sigma Aldrich (USA). All other chemicals were used as received without any further purification.

Modification of Jute Surface

Jute fabrics (J) were first treated with detergent at 70 ºC for 1 h, washed with distilled water and finally dried in a vacuum oven at 70 ºC till attainment of constant weight. Again, de waxing was done by treating with a mixture of alcohol and benzene (1:2) for 72 h at 50 ºC. The fabrics were then treated with 5 % (w/v) NaOH solution for 30 min at 30 ºC and washed with distilled water for several times to leach out the absorbed alkali. Finally, it was immersed in distilled water overnight, washed repeatedly to avoid the presence of any trace amount of alkali. The alkali treated fabrics were dried in a vacuum oven, stored in a desiccator.

Preparation of the slurry

SF powders were mixed with de ionized water in 1:10 ratio (by $^{w}/_{w}$) for 1 h to form a suitable resin containing 5 % glycerol ($^{w}/_{w}$ of dry SF) as a plasticizer. The (SF+Glycerol) slurry was transferred to a round bottom flask. It was stirred for 4 h at 60 ºC with a mechanical stirrer. The temperature of the slurry was then bought down to 35 ºC and GA was added. In order to prepare TNP or TNP - nanoclay filled resin, desired amount of TiO_2 {1 – 5 % ($^{w}/_{w}$ of dry SF)} either alone or in combination with nanoclay (1-5 % $^{w}/_{w}$ of dry SF) was taken in a beaker containing water. It was stirred for 8 h using mechanical stirrer followed by sonication for 30 min and finally added to the slurry containing SF and glycerol. Subsequently the whole resin mixture was stirred for another 1 h followed by sonication for 30 min.

Impregnation of jute fabrics and fabrication of composites

The prepared pre-cured resin slurry was transferred in tray and then surface modified jute fabric was dipped into it. The resultant mixture was allowed to be in room temperature for 24 h. The impregnated jute fabrics were placed in a Teflon coated glass plate, dried in a heating plate at 30-40 ºC for 12 h. The weight of jute fabrics before impregnation is noted as W_1.

Method of film stacking was employed to prepare composite laminates. The layers of impregnated jute fabric were placed on one another having 15 levels in a metal mould of thickness 3 mm. The laminates were then compression moulded at 80 ºC under a pressure of 100 MPa. The laminates were 3 mm in thickness. The final weight of the composite was noted as . The calculations were made as per the following equations:

$$Percentage\ of\ Jute\ in\ the\ Composite = {}^{W_1}/_{W_2} \times 100 \quad (1)$$

$$Percentage\ of\ Resin\ in\ the\ Composite = \left\{{}^{(W_2 - W_1)}/_{W_2}\right\} \times 100 \quad (2)$$

Where, 'W_1' is the weight of jute fabrics before impregnation and 'W_2' is the weight of the final composite.

Measurements

Fourier-transform infrared spectroscopy (FT-IR) study

FT-IR spectra of the composites recorded in FT-IR (Nicolet, Impact 410 spectrophotometer, USA) spectrophotometer.

Scanning Electron Microscopy (SEM) study

The SEM analysis performed using a JEOL scanning electron microscope (model JSM-6390LV) at an accelerating voltage of 15 kV. All the samples were Pt coated before observation.

X-ray diffractometry (XRD) study

XRD measurements were carried out in a Rigaku X-ray diffractometer (Miniflex, UK) using Cu Kα (λ= 0.154 nm) radiation at a scanning rate of 2ºmin-1 with an angle ranging from 2º to 70º.

Transmission electron microscope (TEM) study

The study of the dispersion of TNP alone and in combination with nanoclay particles in the synthesized composite was performed using Transmission Electron Microscope (TEM) (JEOL, JEM 2100) at an accelerating voltage of 200 kV. For TEM investigation, the samples were embedded with epoxy resin. Ultrathin sections (approximately 100 nm thick) of the transverse film surfaces had been sectioned using an ultramicrotome fitted with a diamond knife. The sections were then stained with 1wt% uranyl acetate for sufficient contrast.

Mechanical property study

The tensile and flexural properties of the composites were done in accordance with ASTM D-638 and ASTM D-790 respectively at a crosshead speed of 2 mm min^{-1}. The tensile and flexural strength of the samples measured in Universal Testing Machine-HOUNSEFIELD, England (model H100K-S).

TGA study

Thermogravimetric analysis of the composite samples were done using Shimazdu TGA 50, thermal analyzer under the nitrogen flow rate of 30 mL min-1 at the heating rate of 10 ºC min-1 from 30 ºC to 600 ºC.

Limiting oxygen index (LOI)

LOI values of the samples were measured using flammability tester (S.C. Dey Co., Kolkata) according to ASTM D-2863 method. The ratio of nitrogen and oxygen at which the sample continued to burn for at least 30s was recorded. LOI was calculated as:

$$LOI = \left\{ Volume\ of\ O_2 \Big/ Volume\ of\ (O_2 + N_2) \right\} \times 100 \quad (3)$$

Dimensional stability study

The composites were cut into sizes of 3 mm × 10 mm × 25 mm (radial × tangential × longitudinal) for dimensional stability test. Dimension of oven-dried samples were measured. The samples were then kept in humidity chamber for 72 h at room temperature maintaining relative humidity of 65%. The specimens were taken out from the humidity chamber after stipulated time period and volumes were measured. The percentage of swelling in water vapour was calculated as per formula given below:

$$\%\ Swelling = \left\{ (V_t - V_0) / V_0 \right\} \times 100 \quad (4)$$

Where, ' V_t' is volume of the sample after "t" time and 'V_0' is initial volume of composite sample before water vapour absorption.

UV Resistance Study

The UV degradation study of SF/J composite samples was carried out using a UV chamber (Model S.L.W, voltage, 230 V, power, 1000 W; Advanced Research Co., India) utilizing a mercury arc lamp system that produces a collimated and highly uniform UV flux in the 254−365 nm range. Specimen's dimensions of (25 × 25 × 3) mm^3 were exposed in the UV chamber at room temperature and characterized at specified time intervals. The exposure period was varied from 0 to 60 days. The weight loss was measured using an analytical balance and was calculated as follows: [22]

$$\%\ Weight\ loss = \left\{ (W_t - W_0) / W_0 \right\} \times 100 \quad (5)$$

Where, ' W_t' is the specimen weight at time t, and 'W_0' is the specimen weight before UV exposure. The chemical degradation of the samples was studied by FT-IR where the intensity of the carbonyl (C=O) stretching peaks at 1647 cm^{-1} in SF of the composite was measured. The net peak heights were determined by subtracting the height of the baseline directly from the total peak height. The same baseline were taken for each peak before and after exposure to UV [23]. The SF/J composites degradation was studied by carbonyl index, which was calculated by equation:

$$Carbonyl\ index = I_c / I_R \times 100 \quad (6)$$

Where ' I_C' is the intensity of the carbonyl absorption band (1647 cm^{-1}) and 'I_R ' is the intensity of the reference band (2900-2950 cm^{-1}). This peak was taken to be as reference due to its least change during irradiation. Mechanical properties were also studied after UV exposure.

Results and Discussion

The samples, as coded in Table 1, had been prepared by keeping the weight (%) of the components viz. SF, glycerol, jute and GA constant in all the samples whereas the percentages (%) of TiO_2 and clay nanoparticles were varied. The weight (%) of the different components used for the synthesis of the composite are provided in Table 1.

Table 1: Codification and filler content of the nanocomposites based on Jute and cross-linked SF with TiO_2 nanoparticles and nanoclay (wt %)

Sample	Soy Flour (SF)	Glycerol	Glutaraldehyde (GA)	Jute (J)	TiO_2 (T)	Nanoclay (N)
SF/J/GA50	100	5	50	75	-	-
SF/J/GA50/T1	100	5	50	75	1	-
SF/J/GA50/T3	100	5	50	75	3	-
SF/J/GA50/T5	100	5	50	75	5	-
SF/J/GA50/ T5/N1	100	5	50	75	5	1
SF/J/GA50/ T5/N3	100	5	50	75	5	3
SF/J/GA50/ T5/N5	100	5	50	75	5	-

FT-IR study

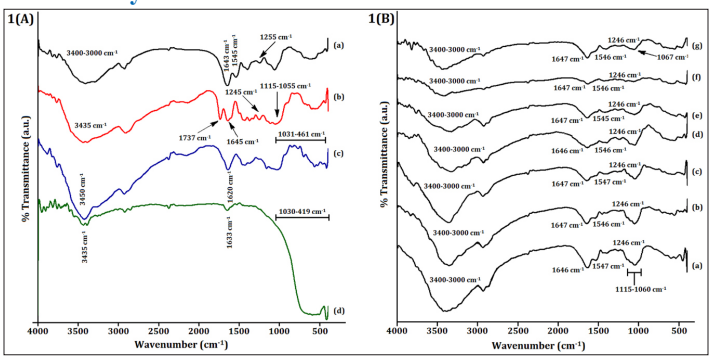

Figure 1: (A) FTIR spectra of (a) soy flour, (b) jute, (c) nanoclay and (d) TiO_2 nanoparticles. (B)FTIR spectra of (a) SF/J/GA50, (b) SF/J/GA50/T1, (c) SF/J/GA50/T3, (d) SF/J/GA50/T5, (e) SF/J/GA50/T5/N1, (f) SF/J/GA50/T5/N3 and (g) SF/J/GA50/T5/N5

Fig. 1 (A) shows the FT-IR spectra of SF, jute, clay, and TNP. The peaks for SF appearedat 1647, 1542 and 1254 cm^{-1} were for C = O stretching of amide – I, – NH bending of amide – II and C – N stretching of amide – III [24]. The absorption bands were observed at around 3440 cm^{-1} for –OH stretching, 1736 cm^{-1} for C=O stretching vibration of ester groups of hemicelluloses, 1643 cm^{-1} for C=O stretching, 1247 cm^{-1} for –C–O–C– bond in cellulose chain and 1057–1116 cm^{-1} for C–O stretchingof jute [18]. Clay (curve-c) show the presence of peaks at 3450 cm^{-1} (–OH stretching), 1619 cm^{-1} (–OH bending) and 1030–460 cm^{-1} (oxide bonds of metals like Si, Al, Mg etc.). FTIR spectrum of TNP (curve-d) shows strong absorbance in the range 1030–419 cm^{-1}due to the Ti–O–Ti stretching of TiO_2. The other notable peaks at 3435 and 1633 cm^{-1} were ascribedto the surface hydroxyl groups of TiO_2 [25,26].

FT-IR spectra for the composite SF/J/GA50, SF/J/GA50/T1, SF/J/GA50/T3, SF/J/GA50/T5, SF/J/GA50/T5/N1, SF/J/GA50/T5/N3, and SF/J/GA50/T5/N5 are presented in Fig. 1B. In all the samples, the peaks were found in the region 3400–3000 cm^{-1}. This could be

due to the –OH and –NH stretching vibrations. In all the spectrum, the characteristic peaks of SF were appeared in the region of 1647, 1542 and 1254 cm^{-1}. Similarly, the peaks assigned for jute were observed at 1247 and 1116–1057 cm^{-1}. The intensities of the peak assigned for –OH and –NH stretching vibrations diminished with respect to unfilled composite suggesting the occurrence of interaction between jute and SF. The intensities of peaks appeared in the region 3400-3000 cm^{-1}decreased with the increase in the concentration of TNP. This could be due to the interaction between the free –OH and –NH groups of jute and SF with –OH groups of TNP. The hydroxyl peak intensities at around 3400 cm^{-1} were found to reduce further on incorporation of clay. The peak intensities in the range of 1030–460 cm^{-1} and 1619 cm^{-1} were found to decrease to a considerable extent. All these suggested active participation of hydroxyl group of clay nanoparticles with S/J/GA50/T composites [27].

SEM study

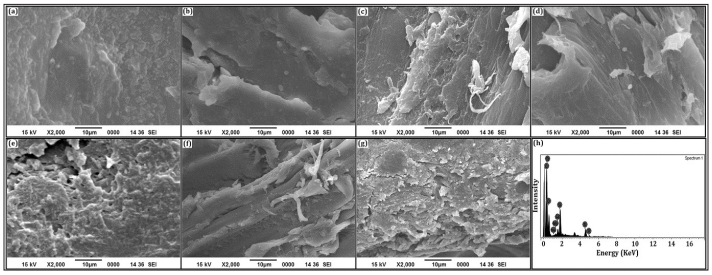

Figure 2: SEM micrographs of (a) SF/J/GA50, (b) SF/J/GA50/T1, (c) SF/J/GA50/T3, (d) SF/J/GA50/T5, (e) SF/J/GA50/T5/N1, (f) SF/J/GA50/T5/N3, (g) SF/J/GA50/T5/N5 and (h) Energy dispersive X-ray analysis of SF/J/GA50/T5/N5

Scanning electron microscopy of fractured surfaces of some selective samples are presented in Fig. 2. The surface of SF/J/GA50sheet was relatively smooth compared to other composites (Fig. 2a). The fractured surface of SF/J/GA50/T1 (Fig. 2b) showed a homogenous structure indicating a relatively uniform distribution of the TNP within the composite. With the increase in the amount of TNP, the fractured surface of the samples (SF/J/GA50/T3 and SF/J/GA50/T5) (Fig 2c, d) became rough due to increase in interfacial adhesion among SF, jute and TNP. The roughness was found to increase further on addition of nanoclay into the TNP loaded nanocomposites (i.e. SF/J/GA50/T5) (Fig. 2e-g). The increase in roughness was due to the increase in interaction caused by the nanoclay with the SF macromolecules and jute fibre [9]. Composite having 3 % nanoclay appeared to be rougher compared to those of the composite prepared with 5 % nanoclay. The agglomeration of clay nanoparticles at higher loading decreased the interaction between the nanoclay and TNP loaded nanocomposites causing a decrease in surface roughness of the composites.

The fractured surface of TNP loaded composites was also used to investigate the energy dispersive X-ray elemental analysis (EDX) simultaneously. Fig. 2h shows the EDX analysis of SF/J composite. The presence of Ti, Al, Na, Si along with C and O confirmed the successful incorporation of TNP and nanoclay into the composite.

XRD study

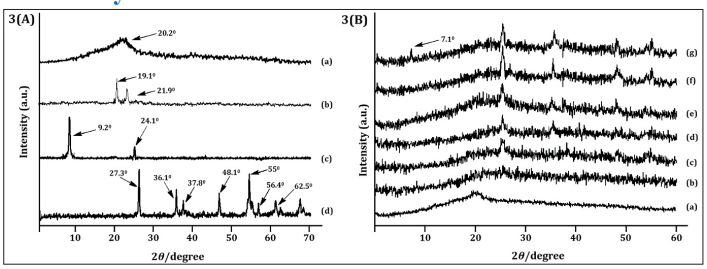

Figure 3: (A) XRD pattern of (a) soy flour, (b) jute, (c) ZnO, and (d) nanoclay. (B) XRD diffractograms of (a) SF/J/GA50, (b) SF/J/GA50/T1, (c) SF/J/GA50/T3, (d) SF/J/GA50/T5, (e) SF/J/GA50/T5/N1, (f) SF/J/GA50/T5/N3 and (g) SF/J/GA50/T5/N5.

Fig. 3A shows the diffractograms of SF, jute, nanoclay, and TNP. Curve-a represents the diffractogram of SF macro molecules. A little shallow peak observed at 2θ = 20.2º suggested the amorphous nature of SF macromolecules. In the diffractrogram of jute (curve-b) the peaks at 2θ = 21.9º and 19.1º were for 002 plane of cellulose I and 101 plane of cellulose II [5]. Curve-c represents the diffractogram of nanoclay. A sharp diffraction peak for nanoclay at 2θ = 9.2º resembling to d-spacing of about 1.2 nm and a small peak at 2θ = 24.1ºwas observed [9]. The anatase as well as rutile phase of TiO_2(curve-d) showed the characteristics peaks at 2θ = 37.8º (004), 48.1º (200), 56.4º (211), and 62.5º (204), and at 27.3º (110), 36.1º (101), 55º (105) [28]. All peaks of bare TiO_2 were in good agreement with the standard spectrum (JCPDS no.: 88-1175 and 84-1286). The diffractograms of SF/J/GA50, SF/J/GA50/T1, SF/J/GA50/T3, SF/J/GA50/T5, SF/J/GA50/T5/N1, SF/J/GA50/T5/N3, and SF/J/GA50/T5/N5 composites are shown in Fig. 3B. In the diffractograms of SF/J/GA50 (i.e. without TNP), a small broad diffraction peak corresponding to jute and SF appeared at around 2θ = 20º (curve-a). The diffractograms of nanocomposites viz. SF/J/GA50/T1, SF/J/GA50/T3, and SF/J/GA50/T5 prepared by varying percentages of TNP (1-5 % w/w of dry SF) are shown in curve (b-d). The peaks corresponding to SF matrix and jute fibre were found in the range 2θ = 19º – 22º. The intensity of the peak appeared due to TNP increased with the increase in the amount of TNP. Mina et al. observed and reported an increase in peak intensity of TiO_2during studying the X-ray diffraction profile of polypropylene/ titanium dioxide composite [29]. The diffraction peaks due to the clay were absent in the composites having 1% and 3% clay (curve e and f). Therefore, it could be inferred that either the clay layers became delaminated or the maximum expansion of clay layers took place, which could not be detected by the XRD. At higher clay loading (SF/J/GA50/T5/N5), an intense peak was observed at 2θ = 7.1º suggesting the occurrence of agglomeration in the composites.

TEM study

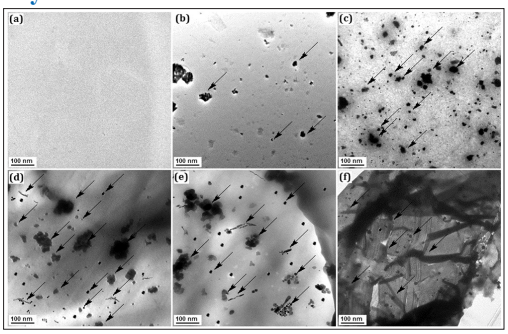

Figure 4: TEM micrograph of (a) SF/J/GA50, (b) SF/J/GA50/T1, (c) SF/J/GA50/T5, (d) SF/J/GA50/T5/N1, (e) SF/J/GA50/T5/N3 and (f) SF/J/GA50/T5/N5

TEM micrographs of the SF/J composites with varying percentage of nanoclay and TNP are shown in Fig. 4. TEM micrographs of composite without TNP and nanoclayis represented by Fig. 4a. The black spots due to TNP were found to appear in TiO_2 containing composite i.e. SF/J/GA50/T1 and SF/J/GA50/T5/N3 (Fig. 4b, c) [21]. The dispersion of nanoclay was observed in SF/J/GA50/T5/N1 and SF/J/GA50/T5/N3 (Fig. 4d, e). The threadlike dark lines and black spots indicated the intersections of the clay layers and TNP. The silicate layers were not distributed homogeneously within the composite suggesting the existence of partial compatibility between jute, polymer, TNP and nanoclay surface [30]. However, at higher concentration of nanoclay, the thickness of dark slices of nanoclay increased due to agglomeration (Fig. 4f). The results obtained from TEM analysis were in good agreement with our XRD findings. Both the results suggest the formation of the partially exfoliated nanocomposites.

Mechanical property study

Table 2.Comparison of Tensile, and Flexural properties of unfilled and filled cross-linked jute based SF nanocomposites before UV treatment

Composite	Tensile Properties		Flexural Properties	
System	Strength (MPa)	Modulus (MPa)	Strength (MPa)	Modulus (MPa)
SF/J/GA50	10.84 (±2.03)	984.3 (±12.66)	15.91 (±1.89)	1777.5 (±11.12)
SF/J/GA50/T1	16.85 (±1.86)	1187.8 (±11.57)	28.98 (±2.23)	2198.9 (±11.43)
SF/J/GA50/T3	28.54 (±1.22)	1819.3 (±12.84)	40.31 (±1.44)	2920.3 (±12.51)
SF/J/GA50/T5	34.25 (±2.68)	1932.4 (±16.11)	49.58 (±2.12)	3631.4 (±12.25)
SF/J/GA50/T5/N1	39.97 (±1.51)	2094.1 (±11.31)	70.93 (±2.54)	4304.5 (±14.57)
SF/J/GA50/T5/N3	55.76 (±1.43)	2443.3 (±12.24)	88.14 (±1.87)	6349.8 (±11.31)
SF/J/GA50/T5/N5	49.13 (±1.32)	2237.8 (±11.75)	79.41 (±2.54)	5866.3 (±12.85)

Each value in the above table represents average of ten samples. Values in the parenthesis represent the standard deviation.

The mechanical properties of SF/J composites reinforced with TNP and nanoclay were studied and reported in Table 2. Both modulus and strength of the composites increased compared to unfilled one due to incorporation of filler. The increase in the percentage of TNP might have direct effect towards the enhancement of mechanical properties of the nanocomposites [21]. Both tensile and flexural properties increased on increasing the TNP content. The enhancement in mechanical properties might be due to the increased interaction between the TNP and cross-linked jute through their hydroxyl groups. The incorporation of clay improved further the mechanical properties. The silicate layers of the nanoclay hold the polymer chains inside their gallery and hindered the movement of polymer chains. Faruk, et al. [31] observed an increase in mechanical properties of wood-plastic composite after the incorporation of nanoclay. The improvement in mechanical properties was found up to 3 % of clay addition, and beyond that, it decreased. At higher percentage of nanoclay, clay particles agglomerated, its interaction with polymer reduced, and as a result, a decrease in mechanical properties were observed. Similarly, higher TNP loading decreased the mechanical properties of the composites due to agglomeration, which was supported by TEM findings.

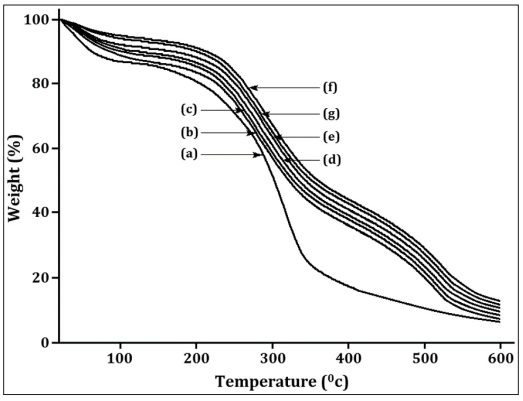

Figure 5: TGAthermograms of (a) SF/J/GA50, (b) SF/J/GA50/T1, (c) SF/J/GA50/T3, (d) SF/J/GA50/T5, (e) SF/J/GA50/T5/N1, (f) SF/J/GA50/T5/N3 and (g) SF/J/GA50/T5/N5

Figure 5 shows the thermograms of SF/J/GA50, SF/J/GA50/T1, SF/J/GA50/T3, SF/J/GA50/T5, SF/J/GA50/T5/N1, SF/J/GA50/T5/N3, and SF/J/GA50/T5/N5. In all the thermograms, an initial weight loss around 100 ºC was observed due to loss of moisture from the composites. All the values (i.e. Ti, Tm, TD& RW%) of the nanocomposites increased with the increase in the amount of TNP. The improvement in thermal stability was due to the heat shielding effect of TNP [32]. On further incorporation of nanoclay, the thermal stability of the TNP loaded nanocomposites were further improved. The silicate layers provided a hindrance to the diffusion of volatile decomposition products. This might also be due to the physico-chemical absorption of the volatile degradation products on the silicate surface of nanoclay. The volatilization of the degraded products originated by carbon-carbon bond scission in the composite was delayed by tortuous path provided by the silicate layers [33]. Laachachi et al. reported that thermal stability of PMMA increased due to the synergistic effect of clay/TiO_2. At higher clay concentration, the agglomeration of clay particles took place and a reduction in the thermal stability was noticed [34]. Therefore, it could be concluded that the thermal stability of SF/J composites was increased on addition up to a certain concentration of TNP and nanoclay.

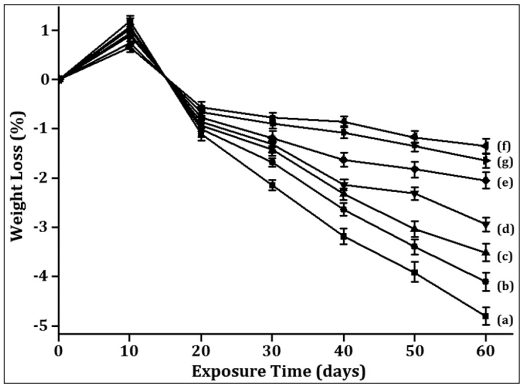

Figure 6. Weight loss vs Exposure time for (a) SF/J/GA50, (b) SF/J/GA50/T1, (c) SF/J/GA50/T3, (d) SF/J/GA50/T5, (e) SF/J/GA50/T5/N1, (f) SF/J/GA50/T5/N3 and (g) SF/J/GA50/T5/N5

The weight loss of SF/J/GA50, SF/J/GA50/T1, SF/J/GA50/T3, SF/J/GA50/T5, SF/J/GA50/T5/N1, SF/J/GA50/T5/N3, and SF/J/GA50/T5/N5 are shown in Fig. 6. Weight losses of different samples were determined at room temperature and found to vary linearly with exposure of time. A small increase of weight was observed initially due to moisture uptake by the composites. This was higher than the material loss induced by the degradation in the initial stage. The percentage of weight loss followed the order: SF/J/GA50/T5/N3 < SF/J/GA50/T5/N5 <SF/J/GA50/T5/N1 < SF/J/GA50/T5 < SF/J/GA50/T3 < SF/J/GA50/T1 <SF/J/GA50. The TNP and nanoclay unloaded composite had shown maximum weight losses. After 60 days of exposure time, the weight losses in S/J/GA50, S/J/GA50/T1, S/J/GA50/T3, S/J/GA50/T5, S/J/GA50/T5/M1, S/J/GA50/T5/M3 and S/J/GA50/T5/M5 were 4.82 ± 0.3 %, 4.09 ± 0.2%, 3.51 ± 0.2 %, 2.96± 0.3 %, 2.03 ± 0.2 %, 1.32 ± 0.1 % and 1.66 ± 0.2 % respectively. The lower weight loss (%) observed for SF/J/GA50/T5/N3 composites on exposure to UV was due to the UV shielding ability of TNP and nanoclay. On exposure to UV radiation, the chain scission and consequently a decrease in the density of the entanglements of the SF polymer chains occurred. This lead to a decrease in the weight of the synthesized composites.

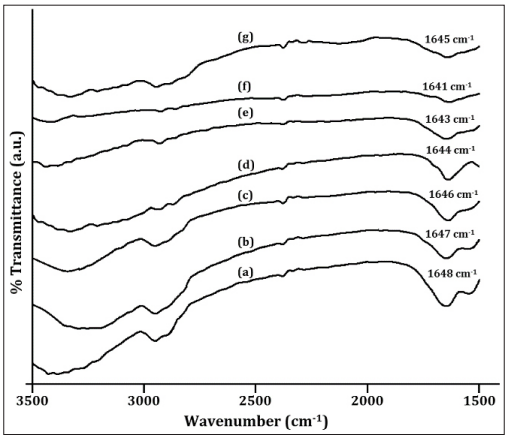

Figure 7: Change in carbonyl peak intensity of (a) SF/J/GA50, (b) SF/J/GA50/T1, (c) SF/J/GA50/T3, (d) SF/J/GA50/T5, (e) SF/J/GA50/T5/N1, (f) SF/J/GA50/T5/N3 and (g) SF/J/GA50/T5/N5

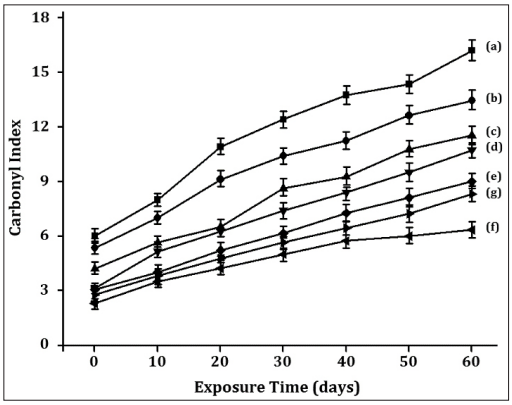

Figure 8: Carbonyl Index value of (a) SF/J/GA50, (b) SF/J/GA50/T1, (c) SF/J/GA50/T3, (d) SF/J/GA50/T5, (e) SF/J/GA50/T5/N1, (f) SF/J/GA50/T5/N3 and (g) SF/J/GA50/T5/N5

Table 3:Changesin the mechanical properties of Unfilled and Filled jute based cross-linked SF nanocomposites after UV Exposure

Composite	Tensile Properties		Flexural Properties	
System	Strength (MPa)	Modulus (MPa)	Strength (MPa)	Modulus (MPa)
SF/J/GA50	4.72 (±1.12)	703.1 (±10.76)	9.88 (±2.07)	1422.2 (±12.45)
SF/J/GA50/T1	9.57 (±1.85)	972.4 (±12.23)	24.79 (±1.76)	1773.3 (±11.34)
SF/J/GA50/T3	22.46 (±1.87)	1641.2 (±11.55)	35.98 (±1.56)	2611.5 (±11.67)
SF/J/GA50/T5	29.63 (±1.21)	1774.3 (±12.12)	44.89 (±1.98)	3276.7 (±12.86)
SF/J/GA50/T5/N1	35.87 (±1.33)	1837.3 (±11.43)	65.88 (±2.18)	3901.2 (±14.34)
SF/J/GA50/T5/N3	52.56 (±1.43)	2152.4 (±15.65)	83.33 (±1.53)	6140.1 (±12.75)
SF/J/GA50/T5/N5	45.89 (±1.23)	1972.3 (±12.79)	74.72 (±2.65)	5564.6 (±11.54)

Each value in the above table represents average of ten samples. Values in the parenthesis represent the standard deviation.

Fig. 7 shows the FT-IR spectra of (a) SF/J/GA50, (b) SF/J/GA50/T1, (c) SF/J/GA50/T3, (d) SF/J/GA50/T5, (e) SF/J/GA50/T5/N1, (f) SF/J/GA50/T5/N3 and (g) SF/J/GA50/T5/N5 after UV exposure. The carbonyl peak intensity was found to enhance after irradiation of the samples for 60 days. Upon exposing the samples to UV-radiation, chain scission of the polymers as well as an increase in the carbonyl index value were observed as depicted in Fig. 8. SF/J/GA50/T5/N3 had lowest carbonyl index value whereas SF/J/GA50 had the highest one. TNP present in the SF/J composites acted as a screen and retarded the photo degradation process. TNP adsorbed the UV radiation and reduced the UV intensity required for the oxidation of the synthesized nanocomposites. The inclusion of TiO_2 improved in UV stability of WF/HDPE composite as reported by Du *et al*. [35].

The existence of nanoclay in the composite also had a screening effect and delayed further photo degradation process. The incorporation of MMT in HDPE improved the UV stability of HDPE [36]. SF/J/GA50/T5/N5 showed lower UV stability compared to SF/J/GA50/T5/N3. This might be due to the agglomeration of nanoclay particles within the composite material. It is well known that UV-radiation has a deterioration effect on many plastic materials. Materials on exposure to outdoor environment undergo photo-degradation and thus causing loss of mechanical properties. Thus, the changes in the mechanical properties of the composites after the UV treatment are presented in Table 3. Flexural as well tensile properties decreased after UV treatment. The loss of mechanical properties of unfilled composites was more compared to nanoparticles filled composites. The maximum loss of mechanical properties was observed for SF/J/GA50.The interfacial interactions among SF, jute, GA, TNP and nanoclays were too strong to decay the massive sheer due to rupture. Hence, the resistance of SF/J composite to UV instability improved significantly by the addition of clay or nanoparticles into the composites.

Dimensional stability study

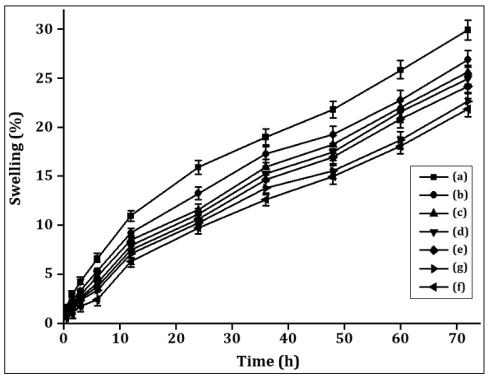

Figure 9: Swelling behaviour of (a) SF/J/GA50, (b) SF/J/GA50/T1, (c) SF/J/GA50/T3, (d) SF/J/GA50/T5, (e) SF/J/GA50/T5/N1, (f) SF/J/GA50/T5/N3 and (g) SF/J/GA50/T5/N5

The water vapour absorption study for different composites was carried out at room temperature (~ 30 ºC) with 65 % relative humidity for different time period shown in Fig. 9. In all the composites, the percentage swelling increased with the increase in time. Water vapour absorption was found to decrease due to the presence of dispersed phase of TNP in the composite materials. Water vapour absorption of S/J/GA50/T composites decreased with the increase in TNP content. TNP provided hindrance to the passage of water due to its strong capability to attract water molecules, and thus reduced the diffusion co-efficient of water. The better the dispersion of TNP in the composite, the higher the retardation of water molecules through it. An increase in barrier property of poly (lactic acid) nanocomposite film after the incorporation of nano-TiO_2 was reported by Zhu *et al*. [37]. Further, the dimensional stability of the SF/J/GA50/T5 composite improved due to incorporation of nanoclay. Silicate layers of nanoclay provided a tortuous path and thus the restricted transport of water molecules through the nanocomposite [9]. Nanoclay at higher concentration (5%) agglomerated within the composite, which resulted in an increase in water vapour absorption capacity.

Limiting oxygen index (LOI) study

Table 4: Limiting Oxygen Indices (LOI) and Flaming Characteristics of the prepared composites.

*Samples	LOI (%)	Flame description	Smoke & Fumes	Char
SF/J/GA50	42 (±0.22)	Small localised flame	Small and black smoke	Little
SF/J/GA50/T1	45 (±0.41)	Small localised flame	Small and black smoke	Higher
SF/J/GA50/T3	49 (±0.63)	Small localised flame	Small and black smoke	Higher
SF/J/GA50/T5	52 (±0.33)	Small localised flame	Small and black smoke	Higher
SF/J/GA50/T5/N1	58 (±0.21)	Small localised flame	Small and black smoke	Higher
SF/J/GA50/T5/N3	68 (±0.42)	Small localised flame	Small and black smoke	Higher
SF/J/GA50/T5/N5	64 (±0.31)	Small localised flame	Small and black smoke	Higher

* Each value represents average five samples.

LOI values of SF/Jute composites with different percentage of TNP and nanoclay are shown in Table 4. All the samples produced small-localised flame and nanoclay filled composites produced higher char than that of the nanoclay free composite. LOI value increased with the increase in the concentration of TNP in the composites. The surface hydroxyl groups of TNP might interacted with SF, jute and GA, forming network structure, thus restricted the transport of oxygen for the production of degradable components from the composites, and hence improved the LOI values [21]. However, on addition of nanoclay into TNP filled composites, further enhancement in LOI value was observed. The introduction of the nanoclay produced a silicate char on the surface of it. The silicate rich surface has better barrier property to heat and oxygen transport due to which ignition of the composite delayed [38]. The LOI value was found to increase upto addition of 3 % of nanoclay. At higher concentration of nanoclay (5 %), the LOI value was found to decrease. At higher clay loading, the aggregation of nanoclay resulted in decrease of interaction with concomitant reduction in barrier property as well as LOI value.

Conclusion

Green nanocomposites consisting of SF, jute, GA, TNP and nanoclay were fabricated using solution induced intercalation method and characterized. The incorporation of TNP improved the physicochemical properties such as mechanical, thermal, flame retardancy, UV-resistance, and dimensional stability *via* interaction of surface hydroxyl group of TNP with hydroxyl group of SF and jute. The composite with 3 % TNP exhibited enhanced physical properties. The incorporation of nanoclay into TiO_2 containing composites resulted in further improvement of the physicochemical properties of the synthesized material. FT-IR study showed a strong interaction among jute fabric, SF, GA, TNP and nanoclay. XRD and TEM studies revealed the distribution of TNP and silicate layers of nanoclay in SF/J composites. Composites containing 5 % TNP and 3% nanoclay showed maximum improvement in physicochemical properties. Thus, TNP in combination with nanoclay could considerably improve the physical properties of natural resources based composites. Consequently, such kind of TNP and nanoclay filled SF/J composites are eco-friendly and may receive applications in newer domains.

References

1. Ma X,Yu J,Kennedy JF (2005) Studies on the properties of natural fibres reinforced thermoplastic starch composites. Carbohydr Polym 62: 19-24.
2. De Rosa IM, Kenny JM, Puglia D, Santulli C, Sarasini F (2010) Morphological, thermal and mechanical characterization of okra (Abelmoschus esculentus) fibres as potential reinforcement in polymer composites. ComposSci Technol 70: 116-122.
3. Sui G, Fuqua MA, Ulven CA, Zhong WH (2010) A plant fiber reinforced polymer composite prepared by a twin-screw extruder. Bioresour Technol 100: 1246-1251.
4. CoatesGW, Hillmyer MA (2009) A Virtual issue of macromolecules: Polymers from renewable resources. Macromolecules 42: 7987-7989.
5. Iman M, Maji TK (2012) Effect of crosslinker and nanoclay on starch and jute fabric based green nanocomposites. CarbohydrPolym 89: 290-297.
6. Espert A, Vilaplana F, Karlsson S (2004) Comparison of water absorption in natural cellulosic fibres from wood and one-year crops in polypropylene composites and its influence on their mechanical properties.Composites Part A 35: 1267-1276.
7. Johnson LA, Myers DJ (1995) Industrial uses for soybeans. In: Erickson DR, editor. Practical Handbook of Soybean Processing and Utilization, AOCS Press, Champaign, IL, USA.
8. Song F, Tang DL, Wang XL, Wang YZ (2011) Biodegradable soy protein isolate-based materials: A review. Biomacromolecules 12: 3369-3380.
9. Iman M, Bania KK, Maji TK (2013) Green jute based cross linked soy flour nanocomposites reinforced with cellulose whiskers and nanoclay. Ind Eng Chem Res 52: 6969-6983.
10. Chabba S, Matthews GF, Netravali AN (2005) Green composites using cross-linked soy flour and flax yarns. Green Chem 7: 576-581.
11. Li H, Huneault MA (2011) Comparison of sorbitol and glycerol as plasticizers for thermoplastic starch in TPS/PLA blends. JApplPolym Sci 119: 2439-2448.
12. Liu D, Chen H, Chang PR, Wub Q, Li K, et al. (2010) Biomimetic soy protein nanocomposites with calcium carbonate crystalline arrays for use as wood adhesive. Bioresour Technol 101: 6235-6241.
13. Sreekumar PA, Gopalakrishnan P, Leblanc N, Saiter JM (2010) Effect of glycerol and short sisal fibers on the viscoelastic behavior of wheat flour based thermoplastic. Composites Part A 41: 991-996.
14. BledzkiAK, Gassan J (1999) Composites reinforced with cellulose based fibres. ProgPolym Sci 24: 221-274.
15. Plackett D, Andersen TL, Pedersen WB, Nielsen L (2003) Biodegradable composites based on l-polylactide and jute fibres. ComposSci Technol 63: 1287-1296.
16. Zaman HU, Khan MA, Khan RA (2012) Comparative experimental measurements of jute fiber/polypropylene and coir fiber/polypropylene composites as ionizing radiation. Polym Compos 33: 1077-1084.
17. Mohanty AK, Misra M, Hinrichsen G (2000) Biofibres, biodegradable polymers and biocomposites. An overview. Macromol Mater Eng 276/277: 1-24.
18. Iman M, Maji TK (2013) Effect of crosslinker and nanoclay on jute fabric reinforced soy flour green composite. JApplPolym Sci 127: 3987-3996.
19. Chieruzzi M, Miliozzi A, Kenny JM (2013) Effects of the nanoparticles on the thermal expansion and mechanical properties of unsaturated polyester/clay nanocomposites. Composites Part A 45: 44-48.
20. Ray SS, Okamoto M (2003) Polymer/layered silicate nanocomposites: A review from preparation to processing. ProgPolym Sci 28: 1539-1641.
21. Deka BK, Maji TK (2011) Effect of TiO_2 and nanoclay on the properties of wood polymer nanocomposite.Composites Part A 42: 2117-2125.
22. Fa W, Yang C, Gong C, Peng T, Zan L (2010) Enhanced photodegradation efficiency of polyethylene-TiO_2 nanocomposite film with oxidized polyethylene wax. JApplPolym Sci 118: 378-384.
23. Stark NM, Matuana LM (2004) Surface chemistry changes of weathered HDPE/wood flour composites studied by XPS and FTIR spectroscopy. PolymDegrad Stab 86: 1-9.
24. Schmidt V, Giacomelli C, Soldi V (2005) Thermal stability of films formed by soy protein isolate-sodium dodecyl sulfat. PolymDegrad Stab 87: 25-31.
25. Zhang SL, Zhou JF, Zhang ZJ, Du ZL, Vorontsov AV, et al. (2000) Morphological structure and physicochemical properties of nanotube TiO_2.Chinese Sci Bull 45: 1533-1536.
26. Xu L, Yang M (2009) In Situ compatibilization between polystyrene-grafted nanosized TiO_2 and polypropylene with friedel-crafts catalyst. JApplPolym Sci 114: 2755-2763.
27. Darder M, Colilla M, Hitzky ER (2003) Biopolymer-clay nanocomposites based on chitosan intercalated in montmorillonite. Chem Mater 15: 3774-3780.
28. Thamaphat K, Limsuwan P, Ngotawornchai B (2008) Phase characterization of TiO_2 powder by XRD and TEM.Kasetsart J (Nat Sci) 42: 357-361.
29. Mina F, Seema S, Matin R, Rahaman J, Sarker RB, et al. (2009) Improved performance of isotactic polypropylene/titanium dioxide composites: effect of processing conditions and filler content. PolymDegrad Stab 94: 183-188.
30. Bendahou A, Kaddami H, Espuche E, Gouanvé F, Dufresne A (2011) Synergism effect of montmorillonite and cellulose whiskers on the mechanical and barrier properties of natural rubber composites.Macromol Mater Eng 296: 760-769.
31. Faruk O, Matuana LM (2008) Nanoclay reinforced HDPE as a matrix for wood–plastic composites.ComposSci Technol 68:

2073-2077.
32. Ansari MO, Mohammad F (2012) Thermal stability of HCl-Doped-Polyaniline and TiO_2 nanoparticles-based nanocomposites. JApplPolym Sci 124: 4433-4442.
33. Pranger L, Tannenbaum R (2008) Biobased nanocomposites prepared by in situ polymerization of furfuryl alcohol with cellulose whiskers or montmorillonite clay. Macromolecules 41: 8682-8687.
34. Laachachi A, Leroy E, Cochez M, Ferriol M, Lopez Cuesta JM (2005) Use of oxide nanoparticles and organoclays to improve thermal stability and fire retardancy of poly(methyl methacrylate). PolymDegrad Stab 89: 344-352.
35. Du H, Wang W, Wang Q, Zhang Z, Sui S, et al. (2010) Effects of pigments on the UV degradation of wood-flour/HDPE composites. JApplPolym Sci 118: 1068-1076.
36. Grigoriadou I, Paraskevopoulos KM, Chrissafis K, Pavlidou E, Stamkopoulos TG, et al. (2011) Effect of different nanoparticles on HDPE UV stability. PolymDegrad Stab 96: 151-163.
37. Zhu Y, Buonocore GG, Lavorgna M, Ambrosio L (2011) Poly (lactic acid)/titanium dioxide nanocomposite films: influence of processing procedure on dispersion of titanium dioxide and photocatalytic activity. Polym Compos 32: 519-528.
38. 38. Camino G, Tartagilione G, Frache A, Manferti C, Costa G (2005) Thermal and combustion behaviour of layered silicate-epoxy nanocomposites. PolymDegrad Stab 90: 354-362.